nature structural & molecular biology

© 2006 Nature Publishing Group http://www.nature.com/nsmb

The FtsK γ domain directs oriented DNA translocation by interacting with KOPS

Viknesh Sivanathan[1,4], Mark D Allen[2,4], Charissa de Bekker[1], Rachel Baker[1], Lidia K Arciszewska[1], Stefan M Freund[2], Mark Bycroft[2], Jan Löwe[3] & David J Sherratt[1]

The bacterial septum-located DNA translocase FtsK coordinates circular chromosome segregation with cell division. Rapid translocation of DNA by FtsK is directed by 8-base-pair DNA motifs (KOPS), so that newly replicated termini are brought together at the developing septum, thereby facilitating completion of chromosome segregation. Translocase functions reside in three domains, α, β and γ. FtsKαβ are necessary and sufficient for ATP hydrolysis–dependent DNA translocation, which is modulated by FtsKγ through its interaction with KOPS. By solving the FtsKγ structure by NMR, we show that γ is a winged-helix domain. NMR chemical shift mapping localizes the DNA-binding site on the γ domain. Mutated proteins with substitutions in the FtsKγ DNA-recognition helix are impaired in DNA binding and KOPS recognition, yet remain competent in DNA translocation and XerCD-*dif* site-specific recombination, which facilitates the late stages of chromosome segregation.

The 4.6-million-base-pair (bp) circular *Escherichia coli* chromosome is replicated bidirectionally from a unique origin (*oriC*), with replication termination occurring in a broad *ter* region opposite *oriC* (reviewed in refs. 1,2). Therefore, replication divides the chromosome into two equal arms or replichores, which locate to separate halves of the *E. coli* cell and behave as units of chromosome segregation[3]. Each replichore is transcribed predominantly in the same direction as replication and contains distinctive asymmetric, base composition–skewed sequences on each strand. These have been implicated in recombination, genome stability and chromosome processing[1,2,4,5]. Separation and segregation of newly replicated sister chromosomes can be compromised by catenation and chromosome dimer formation. Site-specific recombination mediated by the XerCD recombinase occurs between newly replicated sister *dif* sites, located in *ter*, and acts in sister-chromosome segregation by converting any chromosome dimers to monomers and by facilitating decatenation[1,6]. This reaction requires FtsK, a conserved DNA translocase, whose action at the septum coordinates bacterial cell division with the late stages of chromosome segregation. Such coordination underlies faithful chromosome segregation to daughter cells before cell division[2,7]. A closely related translocase, SpoIIIE, pumps chromosomal DNA from the mother cell into the prespore during *Bacillus subtilis* sporulation[8].

A ~200-residue N-terminal integral membrane domain of FtsK functions in cell division and cytokinesis and is linked by a variable-length linker to a ~510-residue C-terminal translocase ($FtsK_C$) that translocates DNA rapidly (~5 kilobases s^{-1} at 25 °C)[9,10]. In *E. coli*, translocation is guided by 8-bp 5′-GGGNAGGG-3′ consensus DNA sequences termed FtsK-orienting polar sequences (KOPS)[11] or FtsK-recognition sequences (FRS)[12]. KOPS are located predominantly on the leading-strand template for replication on each replichore, where they form a pattern of oriented repeated sequences that are polarized from *oriC* to *ter*, with their density increasing as *ter* is approached. KOPS permit DNA translocation by FtsK in one direction and stall translocation in the opposite orientation, with a reverse in direction of translocation observed in single-molecule experiments[10,12]. KOPS-guided DNA translocation by FtsK brings newly replicated *dif* recombination sites to the septum, where FtsK becomes tethered toward the end of DNA replication[13]. Synapsis of sister *dif* sites by FtsK leads to activation of XerCD-*dif* site-specific recombination by a direct interaction between FtsK and XerD[14]. As skewed sequence motifs similar to KOPS are present in most bacterial genomes, guided translocation of DNA by FtsK may operate ubiquitously to facilitate bacterial chromosome segregation.

Structure determinations of $FtsK_C$ with and without DNA have shown that it forms a hexameric ring with a central annulus that accommodates double-stranded DNA[15]. In the structures, the C-terminal 80 amino acid residues (FtsKγ domain; for an overview of the domains, see **Fig. 1**, top) have not been observed, apparently because folded FtsKγ is attached by a flexible linker to the structured αβ motor domain. Although the structures provide insight into the DNA translocation mechanism, they give no clues regarding KOPS recognition by $FtsK_C$ and the way in which this recognition leads to stalling of translocation. Previous studies have demonstrated that FtsKγ interacts directly with the XerCD recombinase bound at the recombination site *dif* to initiate a productive chromosome dimer–resolution reaction[14]. Here, we use a combination of structural and

[1]Department of Biochemistry, University of Oxford, Oxford OX1 3QU, UK. [2]Centre for Protein Engineering and [3]Laboratory of Molecular Biology, Medical Research Council, Hills Road, Cambridge CB2 2QH, UK. [4]These authors contributed equally to this work. Correspondence should be addressed to D.J.S. (sherratt@bioch.ox.ac.uk).

Received 9 June; accepted 27 September; published online 22 October 2006; doi:10.1038/nsmb1158

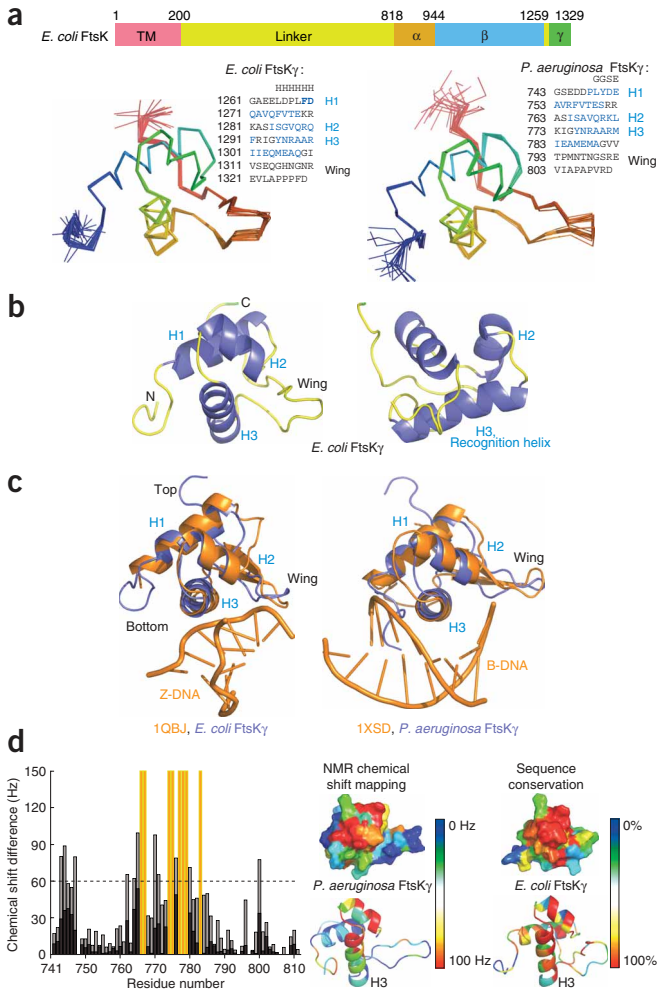

Figure 1 Solution NMR structures of FtsKγ and FtsKγ-DNA binding. (**a**) Ensembles of 20 accepted NMR structures for FtsKγ from *E. coli* (left) and *P. aeruginosa* (right), with annotated protein sequences (for constraints and statistics see **Table 1** and Methods). (**b**) *P. aeruginosa* and *E. coli* FtsKγ form WHDs with helices H1–H3 and the wing. Shown are two views of *E. coli* FtsKγ (rotated 90° around the vertical axis). (**c**) Superposition of FtsKγ and the Zα domain of Z-DNA–bound ADAR1 (PDB 1QBJ, chains B, D and E)[20], the highest DALI[19] hit in the PDB data bank. Superposition highlights a possible DNA-binding surface involving H3 and the wing of FtsKγ. Many, but not all, WHD proteins are involved in DNA binding using the same interface. (**d**) Chemical shift mapping of the DNA-binding surface on *P. aeruginosa* FtsKγ. Left, changes in chemical shift of backbone amide nitrogens (black) and protons (gray) between free and bound (to KOPS-containing 16-bp double-stranded DNA) *P. aeruginosa* FtsKγ (using a 600-MHz spectrometer). Horizontal dotted line indicates an arbitrary 60-Hz cutoff. Assignments for residues 766, 767, 774, 775, 777, 778, 779 and 783 could not be obtained for the DNA-bound protein, owing to an unfavorable chemical exchange regime, and are plotted in gold. Right, structural mapping of the NMR chemical shift data and its relation to sequence conservation. The chemical shift data indicate DNA binding of the γ domain via the tips of helices H3 and H2 and the N-terminal region. For the plot, absent HSQC peaks in the DNA-bound sample were arbitrarily set to 100 Hz. Sequence conservation among γ domains from 251 different species is highest in the same region, consistent with DNA binding.

biochemical methods to reveal that FtsKγ interacts directly with DNA and recognizes KOPS preferentially. Furthermore, we demonstrate that γ acts as a negative regulator of FtsKαβ DNA-translocation activity upon encountering KOPS in the nonpermissive orientation. This work is complemented by that in the accompanying manuscript[16], which demonstrates, by a combination of single-molecule and ensemble studies, that FtsKαβ, lacking the γ domain, is translocation competent yet blind to KOPS.

RESULTS

FtsKγ is a DNA-binding winged-helix domain

Previous studies have shown that the FtsKγ domain is disordered as a whole in crystals containing the αβ and γ domains[15]. *Pseudomonas aeruginosa* FtsK hexamer formation and ATPase activity are negatively and positively affected by the presence of the γ domain in the constructs, respectively. In the same study, it was shown that FtsKγ is folded, as indicated by a widely dispersed ^{15}N-^{1}H HSQC spectrum of the isolated domain. Taking these results together, we conclude that FtsKγ is a separate domain attached via a flexible linker to the hexameric αβ DNA-translocation motor of FtsK, meaning that the motor ring has six loosely attached γ domains located on one side.

To gain insight into the roles of the FtsKγ domains, we solved the structures of both *E. coli* FtsKγ (Met-His$_6$-FtsKγ$_{1261–1329}$) and *P. aeruginosa* FtsKγ (Gly-Gly-Ser-Glu-FtsKγ$_{743–811}$) by solution NMR (**Fig. 1**). ^{15}N labeling was sufficient for structure determination of *E. coli* FtsKγ, whereas *P. aeruginosa* FtsKγ was solved using ^{15}N- and ^{13}C-labeled protein.

E. coli and *P. aeruginosa* FtsKγ form winged-helix domains[17,18] (WHDs, **Fig. 1a**,**b**), containing helices H1, H2 and H3 and the C-terminal wing. We have not assigned or constrained secondary structure in the wing; in other WHD proteins, the wing usually has very few residues in true β-sheet conformation. WHDs are a subtype of helix-turn-helix DNA-binding proteins in which the wing provides additional DNA contacts, typically with the minor groove, during binding of double-stranded B-DNA. In these proteins, the main contact with the major groove of the DNA is facilitated by WHD helix H3 (called the recognition helix; **Fig. 1c**).

Structural similarity searches of *E. coli* FtsKγ using DALI[19] confirmed the similarity to WHD proteins. The top hit, of about 100 WHD proteins, with a *Z*-score of 7.4 (r.m.s. deviation of 2.3 Å over 61 Cα atoms) is PDB 1QBJ, a Z-DNA–binding domain from ADAR1, an RNA-editing enzyme[20] (**Fig. 1c**, left). A DALI search using *P. aeruginosa* FtsKγ revealed that it is most closely related to the dimeric repressor MecI (r.m.s. deviation of 2.4 Å over 64 Cα atoms), which binds palindromic B-DNA[21] (**Fig. 1c**, right). There are many structures with very similar *Z*-scores in these structural similarity searches, reflecting the strong conservation of WHD domains in general and also highlighting the fact that WHD proteins bind a number of different nucleic acid types (B-DNA, Z-DNA and RNA), as well as other proteins. The close relationship of FtsKγ to nucleic acid–binding WHD proteins prompted us to investigate a direct role of FtsKγ in DNA binding and KOPS recognition[17,18].

We therefore performed chemical shift mapping using *P. aeruginosa* FtsKγ to investigate DNA binding and the DNA-binding site (**Fig. 1d** and **Supplementary Fig. 1** online). Initial attempts using *E. coli* FtsKγ proved unsuitable owing to excessive peak broadening. Triply labeled protein was titrated with 16-bp duplex DNA containing KOPS. Some NMR peaks disappeared because of exchange broadening, and this, together with large shifts, clearly indicates the regions of interaction of the protein with DNA. These residues cluster around the tips of helices H3 and H2 and the N terminus (**Fig. 1d**). Only one residue in the wing, Ser800, shows marked changes in chemical shift upon DNA binding. Our interpretation, that the side

© 2006 Nature Publishing Group http://www.nature.com/nsmb

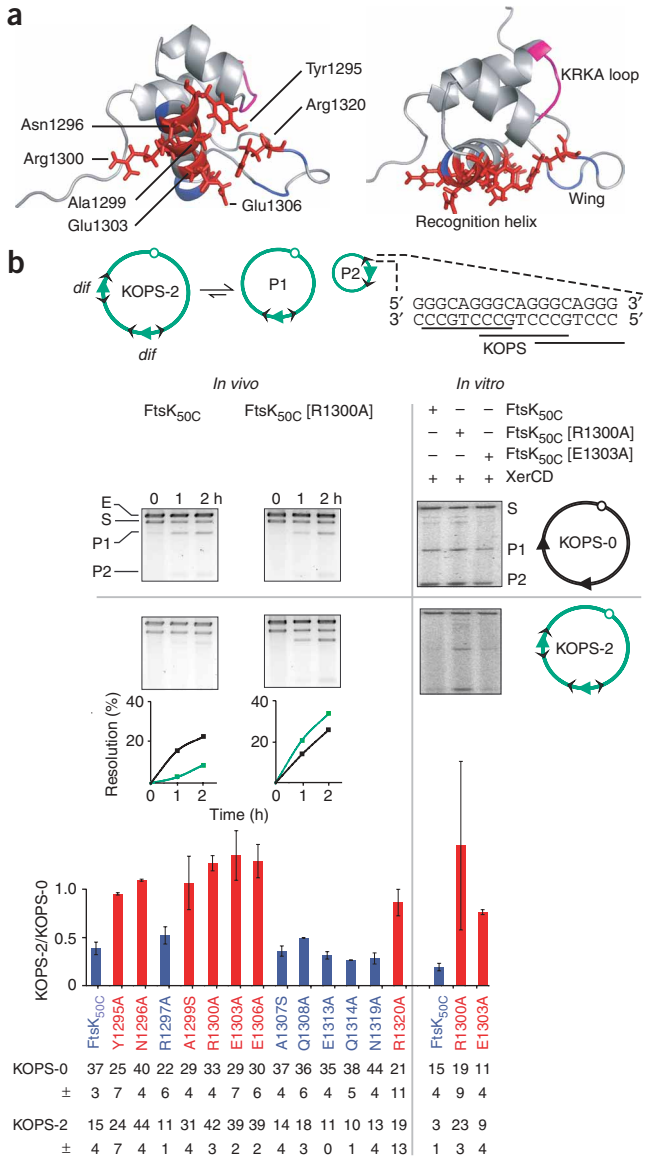

Figure 2 FtsKγ recognizes KOPS. (**a**) Two views of schematic of *E. coli* FtsKγ (residues 1261–1329), showing amino acid residues targeted for mutagenesis. Substitution of side chains shown in red led to loss of KOPS recognition; substitutions in blue had no effect on KOPS recognition. The KRKA loop that interacts with XerD is shown in magenta[14]. (**b**) *dif* recombination assays. The KOPS-0 plasmid is a pSC101 derivative carrying two directly oriented *dif* sites separated by a kanamycin resistance gene cassette[14]. XerCD recombination generates two circular molecules, only one of which can replicate *in vivo*. The KOPS-2 plasmid is the same as KOPS-0, other than having three overlapping KOPS sequences in the nonpermissive orientation on both sides of each *dif* site. Top diagram, recombination reaction. Gels show *in vivo* data (left) for $FtsK_{50C}$ and $FtsK_{50C}$[R1300A], and *in vitro* data (right) for $FtsK_{50C}$, $FtsK_{50C}$[R1300A] and $FtsK_{50C}$[E1300A]. S, substrate; P1, P2, products; E, plasmid expressing the $FtsK_{50C}\gamma$ variant. *In vivo* results are plotted below gels: black, KOPS-0 recombination; green, KOPS-2 recombination. Histogram shows ratios of KOPS-2 recombination to KOPS-0 recombination by $FtsK_{50C}\gamma$ variants. KOPS-blind mutants (red) are defined as having less than 25% reduction in recombination on KOPS-2 as compared to KOPS-0. Values below chart show means and s.d. from two independent experiments.

of FtsKγ that has helices H3 and H2 protruding is involved in DNA binding, is further strengthened by an extensive sequence alignment of 251 FtsKγ domains (**Fig. 1d**, right). The clusters of large changes in chemical shift upon DNA binding are in exactly the same place as regions of high sequence conservation. The NMR FtsKγ-DNA titration experiments showed that complex formation is in the fast-to-intermediate timescale, consistent with a K_d for the FtsKγ-DNA interaction in the low micromolar range (data not shown).

E. coli FtsKγ recognizes KOPS DNA

To explore FtsKγ-DNA binding and KOPS recognition, the recognition helix H3 and the wing were targeted for mutational analysis in a biochemically tractable *E. coli* $FtsK_{50C}$ derivative[22]. Thirteen amino acid residues in the recognition helix and the wing were substituted individually (**Fig. 2a**). Initially, the mutant proteins were screened *in vivo* for KOPS recognition. This assay assessed the ability of the variants to support XerCD recombination between directly repeated *dif* sites in plasmid substrates that either lacked KOPS (KOPS-0; control) or had pairs of KOPS in a nonpermissive orientation bounding both *dif* sites (KOPS-2; **Fig. 2b**). All 13 derivatives showed at least 50% of wild-type XerCD-*dif* recombination activity on the KOPS-0 substrate and could therefore still translocate and interact productively with XerD. The wild-type $FtsK_C$ domain present in $FtsK_{50C}$ recombined the KOPS-2 substrate at a lower level (39% ± 7%) than KOPS-0, presumably because the translocase did not efficiently access the *dif* sites bounded by nonpermissive KOPS. Of nine variants with mutations in H3, six (red in **Fig. 2**) were blind to KOPS and supported maximal recombination on the KOPS-2 restricted substrate; one of the four wing variants (R1320A, red), whose mutation is at the end of the wing loop, was also KOPS-blind. Arg1320 is invariant in all FtsK proteins, and the side chain of this residue is in close proximity to Glu1303, which is one of the six residues in H3 that seem to be involved in DNA binding. Arg1320 and Glu1303 probably form a salt bridge, which might explain the absence of a large signal from the residue equivalent to Arg1320 in the *P. aeruginosa* FtsKγ NMR chemical shift mapping. Note that the adjacent residue, *P. aeruginosa* Ser800 (equivalent to *E. coli* Asn1319) is directly involved in DNA binding, as assessed by chemical shift, although substitution of *E. coli* Asn1319 by alanine did not ablate KOPS recognition.

Two of the KOPS-blind mutants, in which the original residue is invariant (Arg1300) or highly conserved (Glu1303), were tested for KOPS recognition *in vitro*, using the XerCD-*dif* recombination assay on KOPS-0 and KOPS-2 plasmids (**Fig. 2b**, right panels). The *in vitro* recombination assay mirrored the results *in vivo*. Both mutants recombined KOPS-2 and KOPS-0 substrates with similar efficiency, whereas the wild-type protein showed an even stronger KOPS selectivity than *in vivo*. The products of all recombination reactions were free circles rather than catenated circles, confirming the DNA-translocation competence of these mutants[7] (data not shown).

Translocation and KOPS recognition of $FtsK_{50C}$ γ variants were also examined directly in a triplex displacement assay using a 2.9-kbp DNA substrate in which access to the triplex, located close to one end, was restricted by two nonoverlapping KOPS placed 60 bp internal to the triplex (**Fig. 3**). Translocation of $FtsK_{50C}$ was impeded by KOPS in the nonpermissive orientation, with the initial, rapid rate of displacement being 36% ± 8% of that in the permissive orientation. This modest reduction of translocation is consistent with previous studies that show a ~40% probability of translocation through each copy of nonpermissive KOPS[12].

© 2006 Nature Publishing Group http://www.nature.com/nsmb

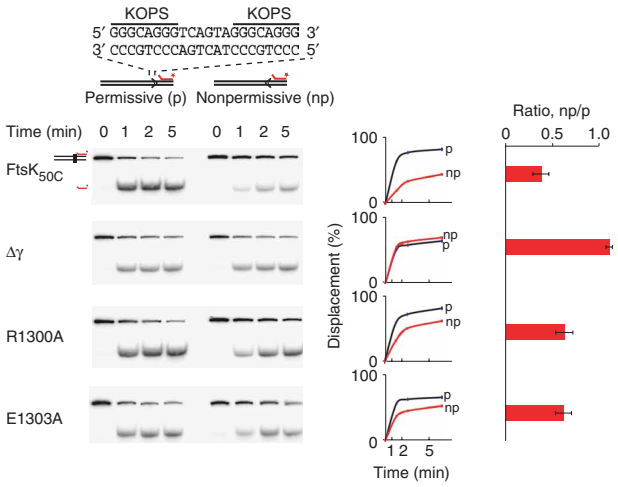

Figure 3 KOPS recognition determined by triplex displacement. The 2.9-kb DNA substrate contained a triplex-forming sequence 15 bp from one end. Substrate variants contained KOPS in either permissive (p) or nonpermissive orientation (np) 60 bp from the triplex-forming site. Displacement of a ^{32}P 5′ end–labeled triplex-forming oligonucleotide carrying a 4-nucleotide flap at its 3′ end (red line with star in diagrams) was monitored for 5 min. Histogram shows ratios of displacement on nonpermissive to displacement on permissive substrates (mean and s.d. from two independent experiments).

FtsK$_{50C}$ lacking γ (Δγ) displaced the triplex oligonucleotide with a rate that was similar to that of FtsK$_{50C}$ and indistinguishable in the two KOPS orientations. Therefore, the αβ motor is sufficient, as well as necessary, for maximal rates of DNA translocation, whereas FtsKγ downregulates αβ motor activity through its interaction with KOPS in the nonpermissive orientation. Both KOPS-blind mutants tested also displaced the triplex efficiently from the nonpermissive substrate, although both showed evidence of residual KOPS recognition, as the initial rates were reduced to 61% ± 9% in the nonpermissive orientation, as compared to the control.

KOPS selectivity in the interaction of FtsKγ with DNA

To provide further insight into how FtsKγ interacts with DNA and recognizes KOPS, we constructed His-tagged variants of FtsKγ (residues 1261–1329) carrying the KOPS-blind mutations R1300A and E1303A, and we analyzed their ability to interact with DNA using an electrophoretic DNA band–shift assay. The wild-type FtsKγ formed complexes with 20-bp DNA fragments carrying three overlapping KOPS (tKOPS; **Fig. 4a**). This substrate was used to maximize any preferential interactions with FtsKγ[12] and to minimize nonspecific DNA interactions, as there is only 1 bp of nonspecific DNA at each end of the fragment.

Despite remaining fully active in stimulating XerD-mediated cleavage of a *dif*-BSN cleavage substrate[14], indicating that they are folded and have biological activity, the mutated proteins did not form complexes with tKOPS that could survive electrophoresis (**Fig. 4a**). Furthermore, DNA fragments lacking KOPS formed no detectable complexes with the γ mutants (data not shown), although complexes with the wild-type protein were observed (**Fig. 4b**). Therefore, Arg1300 and Glu1303, located within H3, must be important for stable interactions with DNA, irrespective of the presence of KOPS, consistent with H3 being the DNA recognition helix.

Comparison of binding of FtsKγ to KOPS and non-KOPS DNA was assessed by band-shift assays and gel filtration. Titration and competition experiments using band-shift assays were used to assess any preferential FtsKγ binding to KOPS. Radiolabeled 20-bp fragments that lacked KOPS (nKOPS) or that contained a single KOPS (sKOPS)

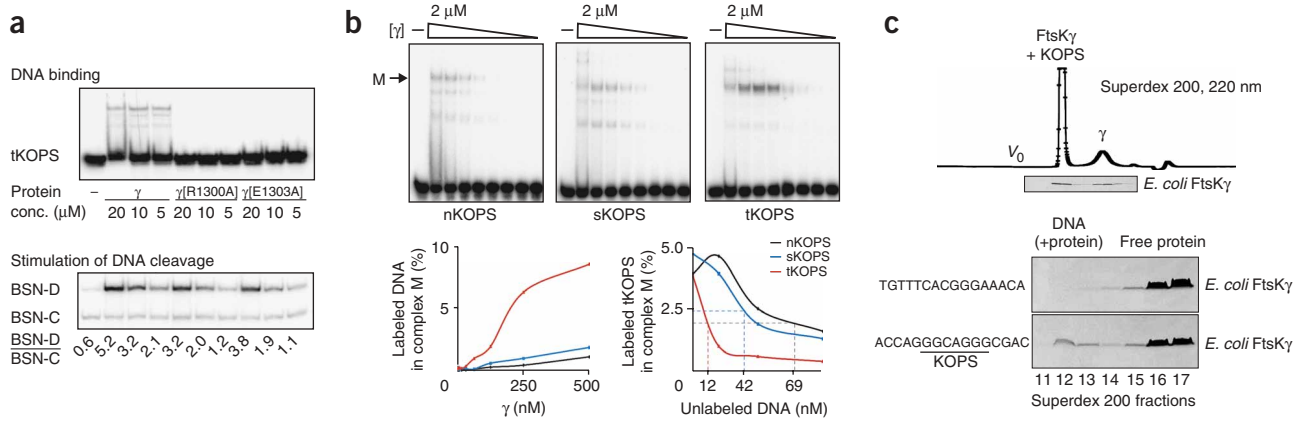

Figure 4 FtsKγ binds KOPS DNA preferentially. (**a**) DNA-binding analysis of KOPS-blind variants. Top, DNA duplexes (20 bp) carrying three overlapping KOPS (tKOPS) or lacking KOPS (nKOPS) were incubated with FtsKγ or its variants at the indicated concentrations. Bottom, folding and biological activity of the variants (concentrations as in top gel) were tested by their ability to stimulate *dif*-BSN DNA cleavage by XerD. BSN-D and BSN-C are covalent DNA recombinase products of XerD- and XerC-mediated cleavage, respectively. Ratios of cleavage by XerD and by XerC (below) quantify the level of γ stimulation of DNA cleavage by XerD[14]. (**b**) Binding of γ to nKOPS, sKOPS and tKOPS DNA substrates. The concentration of γ in the reactions analyzed decreased by two-fold steps from ~2 μM (triangles denote decrease). Left plot shows percentage of substrate DNA in the major protein–DNA complex, M, as a function of γ concentration. Right plot shows competition for binding of γ to KOPS; radiolabeled tKOPS substrate (2 nM) was incubated with γ (2 μM) in the absence or presence of increasing amounts of unlabeled tKOPS, sKOPS and nKOPS DNA. Dotted lines indicate concentrations of unlabeled DNA that decrease labeled complexes two-fold. (**c**) Superdex 200 gel filtration of *E. coli* FtsKγ in the presence of DNA. V_0, excluded volume. Top, most *E. coli* FtsKγ was complexed with KOPS in an experiment with a 4:1 molar ratio of *E. coli* FtsKγ to KOPS. Bottom, only DNA containing KOPS formed a complex with *E. coli* FtsKγ (FtsKγ/KOPS, 13-fold molar excess; FtsKγ/non-KOPS, 12-fold molar excess). SDS-PAGE of indicated fractions is shown. The *E. coli* FtsKγ–KOPS complex contains an average of ~3:1 (molar) protein/KOPS.

© 2006 Nature Publishing Group http://www.nature.com/nsmb

© 2006 Nature Publishing Group http://www.nature.com/nsmb

or three overlapping KOPS (tKOPS) were incubated with increasing concentrations of γ. Note that the 20-bp sKOPS fragment contains 12 bp of non-KOPS sequence; smaller sKOPS fragments lacking random DNA are too unstable to survive gel electrophoresis.

With each of these fragments, we observed a major highly shifted band (M) and other minor faster-migrating bands, along with smearing at the highest protein concentrations (**Fig. 4b**, top). When γ-binding was assessed, the amount of shifted DNA increased as a function of protein concentration, irrespective of whether band M (**Fig. 4b**, bottom left) or the integrated amount of all shifted protein–DNA complexes (data not shown) was quantified. Comparison of binding to tKOPS and nKOPS indicates a five- to ten-fold higher binding affinity to tKOPS, with an intermediate value for sKOPS, consistent with the observation that, in nonpermissive orientation, tKOPS provides a stronger barrier to FtsK translocation than sKOPS[12]. The greatest selectivity for KOPS binding was observed for the complex present in band M. We believe that the different shifted bands reflect largely binding between DNA and FtsKγ molecules of different oligomeric states. Concentration-dependent FtsKγ oligomerization in solution precludes the determination of a precise K_d for the interaction between FtsKγ and KOPS or random DNA. Nevertheless, we believe our conclusion from this experiment, of preferential KOPS binding, is robust. The results below strengthen this conclusion. Furthermore, we note that any K_d determined *in vitro* will have little relevance to the *in vivo* situation where six γ domains tethered to a FtsK hexamer are available for KOPS-DNA interaction.

We next added increasing quantities of unlabeled tKOPS, sKOPS or nKOPS DNA to compete with the binding of γ to radiolabeled tKOPS DNA. The concentration of unlabeled nKOPS DNA required to reduce the amount of labeled FtsKγ–tKOPS complexes by a factor of 2 was about six times higher than the amount of unlabeled tKOPS DNA required to give the same two-fold reduction in labeled FtsKγ–tKOPS complexes. Again, this is consistent with a modest selectivity for KOPS binding (**Fig. 4b**, bottom right).

In gel filtrations, when *E. coli* FtsKγ was present in a four-fold molar excess over a 16-bp fragment containing a single KOPS, most of the protein migrated as a defined protein–DNA complex (**Fig. 4c**, left). Selectivity in binding the 16-bp KOPS fragment as compared to a 16-bp random DNA sequence was evident even when the protein excess was increased to 12- to 13-fold; FtsKγ–DNA complexes were observed with KOPS but not with random DNA (**Fig. 4c**, right). By measuring protein and DNA concentrations in concentrated fractions containing the defined complex, we estimate that approximately three FtsKγ domains bind one duplex of 16-bp KOPS DNA under these conditions; 20 ± 2 mg ml^{-1} protein was bound to 7.7 ± 1 mg ml^{-1} DNA, giving a molar ratio of 3.3:1.

Together, the three experiments lead us to conclude that FtsKγ interacts with DNA with a modest selectivity for KOPS. Furthermore, the results from NMR chemical shift mapping and the mutational analysis both identify FtsKγ H3 as having a key role in DNA interactions, consistent with γ being a WHD family member.

DISCUSSION

FtsKγ regulates FtsKαβ motor activity

Our data demonstrate that FtsKαβ comprises an ATP hydrolysis–dependent, DNA sequence–independent motor whose activity can be downregulated when FtsKγ interacts with KOPS in the nonpermissive orientation.

WHDs are predicted to be present on the C-terminal side of the catalytic domains of several AAA^+ ATPases[18]. In the case of archaeal Orc/cdc6 proteins, the WHD has been shown to be necessary for DNA binding and origin recognition. The location of this domain relative to the catalytic domain has been proposed to be a regulatory switch dependent upon the nucleotide binding state of the protein[23]. Additionally, a C-terminal WHD has been implicated in DNA interactions, but not catalytic DNA motor activity, in RuvB, which branch-migrates Holliday junction–containing DNA[24]. We speculate that the WHDs present at the C termini of at least some ring-shaped AAA^+ ATPases that interact with DNA may generally regulate DNA motor activity. For example, it may be advantageous to switch off the activity of mini-chromosome maintenance (MCM) proteins when awaiting origin firing or during replication, while retaining the ability to rapidly restart activity. A regulatory switch, akin to that proposed here for FtsKγ, would be an attractive solution.

As FtsKγ interacts with KOPS and with the XerCD site-specific recombination machinery, it seems possible that each of these interactions leads to a stalling of translocation by the same mechanism. Because the selectivity of FtsKγ binding for KOPS over random DNA is modest, at least in binding assays *in vitro* when the domain is not attached to hexameric motor domains, we suspect that the interaction of γ and KOPS does not apply a strong 'brake' that halts translocation; translocation has a stall force of >65 pN in single-molecule experiments[10]. When six γ domains are bound to the FtsK motor domains via the flexible linker, they will be present at a very high local concentration that may change apparent affinities and selectivities drastically. This could explain, in part, the differences seen with the triplex-displacement and DNA band–shift assays: residual KOPS selectivity is present in the mutants (R1300A and E1303A) of hexameric $FtsK_{50C}$ when assayed by triplex displacement, whereas no DNA binding is seen with the band-shift assays using the isolated FtsKγ domain.

We consider three plausible mechanisms for the modulation of motor activity by FtsKγ. (i) KOPS adopts a specific DNA configuration upon interaction with FtsKγ, and this leads to transduction of a signal to αβ through the DNA. Such a mechanism would not necessarily require that FtsKγ be covalently attached to αβ. We note that KOPS is a good match to a G-quartet consensus[25], but do not see how G-quartet formation could be simply implicated in FtsK stalling upon interaction with KOPS. Alternatively, KOPS may adopt the left-handed Z-DNA configuration upon binding to γ, a situation observed in other WHD-DNA interactions[20] (for example, see **Fig. 1c**). The formation of Z-DNA could stall DNA translocation because the phosphate backbone is distorted, and it could be envisaged that the rotary inchworm mechanism of translocation would stop when Z-DNA was encountered. However, we note that the interactions revealed here between γ and DNA are more similar to those of WHD proteins and B-DNA. (ii) Interaction of KOPS with FtsKγ leads to inhibition of αβ ATPase as a consequence of allosteric changes in protein conformation or through some mechanical transduction through the protein. This could lead to a change in the conformation of the nucleotide-binding pocket, which is positioned close to the expected interface of γ and αβ. This seems feasible, as the γ domain is attached to the αβ motor domain via a loop and helix that are in direct contact with the nucleotide[15] (residues 693–722 in *P. aeruginosa* FtsK). (iii) The same interactions may cause a more global change in αβ, leading, for example, to a destabilization of the hexameric structure. This would be consistent with the observation that the presence of γ makes FtsKαβ hexamer formation more difficult[15]. Ongoing structural and biochemical studies of FtsK–DNA complexes should provide insights into the mechanisms of motor activity and directionality and the motor direction reversal seen in single-molecule studies.

The FtsKγ residues involved in DNA binding and KOPS recognition are almost invariant among all known FtsKs, whereas natural variation is rather common at the other positions that were mutated (**Fig. 1d** and **Fig. 2a**). This is consistent with KOPS providing a universal mechanism in eubacteria for securing overall directionality of the FtsK translocation motor. This motor can assemble randomly in either orientation on DNA segments and has a key role in coordinating chromosome segregation, sporulation and cell division. Directionality mechanisms that use oriented DNA within a chromosome to direct the global action of protein machines that can assemble in different orientations may be used widely in biological systems.

METHODS

Bacterial strains. *In vivo* assays for FtsK function used *E.coli* DS9041 *ftsK*::*cat1*, which expresses the essential N-terminal domain of FtsK[25]. Proteins for functional studies were purified from DS9040, which lacks functional *xerC* and *xerD* genes[14]. Variants of *E. coli* $FtsK_{50C}$ were purified from DS9041.

Recombinant proteins. N-terminal Flag epitope–tagged *E. coli* $FtsK_{50C}$, $FtsK_{50C}\alpha\beta$ and $FtsK_{50C}\gamma$ variants were expressed from the arabinose promoter of plasmid pBAD24 (ref. 26) and purified on M2 anti-Flag agarose affinity gel (Sigma). FtsKγ and its variants were expressed as N-terminal His-tag fusions cloned in pBAD24 (pRB238, producing *E. coli* FtsKγ, with sequence Met-His_6-$FtsK\gamma_{1261–1329}$). *E. coli* FtsKγ purification involved three chromatographic steps: nickel resin, diethylaminoethyl Sepharose and HiTrap S (GE Healthcare). Purification of His-tagged *E. coli* FtsKγ variants was by one step, using nickel-resin separation. XerC and XerD proteins were purified as reported[27,28]. *P. aeruginosa* FtsKγ was expressed as an N-terminal His-tag fusion protein cloned into a modified pRSETA vector (pHLTV-PAKG, producing *P. aeruginosa* FtsKγ, with sequence Gly-Gly-Ser-Glu-$FtsK\gamma_{743–811}$).

Large-scale expression, purification and labeling of *E. coli* FtsKγ. Plasmid pRB238 was transformed into BL21(AI) cells, which were grown in 120 l of culture in a New Brunswick Bioflo Pro fermentor and induced with 0.2% (w/v) arabinose. Protein from 500 g of cells was purified using nickel Sepharose FF (GE Healthcare, imidazole elution), ammonium sulfate precipitation, SP Sepharose HP (NaCl elution) and Sephacryl S-100. Storage buffer was 20 mM Tris-HCl, 200 mM NaCl, 1 mM EDTA and 1 mM sodium azide (pH 7.5). Protein identity was checked using electrospray mass spectrometry: measured mass was 8665 Da; calculated mass including N-terminal methionine is 8665 Da. We obtained 40 mg protein from 120 l culture. For ^{15}N labeling, M9 medium with ^{15}N ammonium chloride, supplemented with minerals and vitamins, was used and the protein was purified as above from 50 l culture. NMR buffer was 20 mM potassium phosphate and 150 mM sodium chloride (pH 6.5).

Expression, purification and labeling of *P. aeruginosa* FtsKγ. Plasmid pHTLV-PAKG was transformed into C41 cells. The fusion protein was initially purified by Ni^{2+}-chelating sepharose affinity chromatography. Subsequent tobacco etch virus protease digestion, dialysis and Ni^{2+}-chelating sepharose affinity chromatography removed the lipoyl domain fusion tag. The *P. aeruginosa* FtsKγ domain was further purified by Source Q ion-exchange chromatography (NaCl elution). Protein identity was checked using electrospray mass spectrometry. We obtained 40 mg of protein from 2 l culture. Two isotopically labeled *P. aeruginosa* FtsKγ proteins were made, both using K-MOPS minimal medium supplemented with minerals and vitamins. One contained 20 mM $[^{15}N]NH_4Cl$, 0.4% (w/v) $[^{13}C]$glucose and 85% (v/v) D_2O. The other contained 20 mM $[^{15}N]NH_4Cl$, 0.04% (w/v) $[^{13}C]$glucose and 0.36% (w/v) $[^{12}C]$glucose. NMR buffer was 20 mM Tris, 100 mM sodium chloride and 1 mM sodium azide (pH 7.0).

Spectroscopic measurements. All NMR spectra were recorded on Bruker Advance-800, Advance-600 and DMX-500 spectrometers. 2D NOESY, TOCSY, DQF-COSY, ^{15}N-HSQC and ^{13}C-HSQC (natural abundance), and 3D HNHB, ^{15}N-NOESY, ^{15}N-TOCSY spectra of *E. coli* FtsKγ domain were recorded at 298 K. 2D NOESY, TOCSY, DQF-COSY, ^{15}N-HSQC and constant-time ^{13}C-HSQC (uniformly labeled and 10% (w/w) ^{13}C-labeled), and 3D HNCACB, CBCACONH, HNCO, HNCACO, HNHB, ^{15}N-NOESY, ^{15}N-TOCSY spectra of the *P. aeruginosa* FtsKγ domain were recorded at 293 K. The mixing times chosen were 55 ms for TOCSY and 100 ms for NOESY. Spectra were referenced relative to external sodium 2,2-dimethyl-2-silapentane-5-sulfonate for signals of proton and carbon, or liquid ammonium for that of nitrogen.

The resonances of *E. coli* FtsKγ were assigned by standard 2D procedures[29] using both unlabeled and uniformly ^{15}N-labeled *E. coli* FtsKγ. Approximately half of the Hβ resonances were assigned stereospecifically using a combination of HNHB and DQF-COSY spectra. The backbone and some of the side chain resonances of *P. aeruginosa* FtsKγ were assigned by standard triple-resonance procedures using a uniformly ^{15}N,^{13}C-labeled sample, whereas additional side chain resonances were assigned by standard 2D procedures[29] using both unlabeled and uniformly ^{15}N-labeled *E. coli* FtsKγ . All of the valine Hγ and leucine Hδ resonances of the *P. aeruginosa* FtsKγ domain were assigned stereospecifically using a 10% (w/w) ^{13}C-labeled sample[30]. All NMR spectra were analyzed with ANSIG v3.3 (ref. 31). For hydrogen-exchange experiments, lyophilized ^{15}N-labeled FtsKγ was exchanged into NMR buffer containing 100% (v/v) D_2O, and a series of ^1H-^{15}N HSQC spectra were recorded over the course of 24 h. Additional stereospecific assignments were identified for resolved resonances only when the side-chain atoms were sufficiently well defined in the ensemble of structures.

Structure determination. 2D ^1H-^1H NOESY and 3D ^1H-^{15}N spectra were integrated according to the cross-peak strengths and calibrated by comparison with NOE connectivities obtained for standard inter-residue distances within an α-helix. The distance constraints derived from the NOESY spectra were classified into four categories corresponding to interproton distance constraints of 1.8–2.8, 1.8–3.5, 1.8–4.75 and 1.8–6.0 Å, respectively. Torsion-angle constraints were obtained from stereospecific assignment of residue side chains and incorporated in the structure calculation, along with the backbone φ and ψ angle constraints determined with TALOS[32]. The structures were calculated by a standard torsion-angle dynamics simulated annealing protocol using CNS[33]. Stereospecific constraints were incorporated where intraresidue and sequential NOEs agreed with the calculated structures. Hydrogen bond constraints were included for a number of backbone HN groups whose signals were observed to change slowly when the sample buffer was exchanged for D_2O. Hydrogen bond acceptors were identified in the last round of structure calculations from an ensemble of accepted structures. Hydrogen bond constraints of 1.8–2.1 Å were imposed on the distance between the hydrogen and the acceptor oxygen, whereas another constraint of 2.7–3.1 Å was imposed on the distance between the donor nitrogen and the acceptor oxygen. For the final structural ensemble, we chose the 20 lowest-energy (total energy) structures where no distance violations were >0.25 Å and no angle violations were $>5.0^\circ$. A Ramachandran plot of the final 20 structures of *E. coli* FtsKγ showed 90.0%, 8.8%, 0.3% and 0.0% of residues in the most favored, allowed, additional allowed and disallowed regions, respectively. A Ramachandran plot of the final 20 structures of *P. aeruginosa* FtsKγ showed 88.0%, 10.9%, 0.8% and 0.3% of residues in these regions, respectively. See **Table 1** and **Supplementary Figure 2** online.

NMR chemical shift mapping. The DNA-binding site was localized by monitoring the changes in the 2D ^1H-^{15}N HSQC spectra of the *P. aeruginosa* FtsKγ domain upon the addition of a 16-bp KOPS DNA duplex (5′-ACCAGGGCAGGGCGAC-3′). DNA binding altered the NMR spectrum of the domain (**Supplementary Fig. 1**). A number of peaks changed chemical shift, others decreased in intensity and some disappeared. NMR-monitored titrations indicated that the peaks that changed chemical shift are in the fast-exchange regime relative to the chemical shift time scale. The peaks that disappeared presumably undergo larger changes in chemical shift upon binding and are in the intermediate regime.

***In vivo dif* plasmid recombination.** We used pFX142 (KOPS-0)[14] and its derivative, KOPS-2, as substrates in *dif* recombination assays[34]. Exponentially growing DS9041 cells carrying vectors expressing $FtsK_{50C}$ variants and one of the *dif* resolution plasmids were induced with arabinose (0.01% w/v). Plasmid DNA extracted from cells harvested after 0, 1 or 2 h was analyzed by agarose gel electrophoresis (1% w/v, in TAE). The gels were stained with Sybr Green and analyzed in a Fuji FLA3000 fluorimager.

© 2006 Nature Publishing Group http://www.nature.com/nsmb

***In vitro dif* plasmid recombination.** *In vitro* plasmid-resolution reactions (20 µl, 37 °C, 1 h) were in 50 mM HEPES (pH 7.5), 50 mM potassium glutamate, 10 mM $MgCl_2$ and 5% (w/v) glycerol and contained 5 nM plasmid DNA, 250 nM FtsK, 250 nM XerC, 125 nM XerD and 5 mM ATP. Reactions were stopped by proteinase K, EDTA and SDS. Reacted DNA was separated on a 1% (w/v) agarose gel containing TAE.

Triplex displacement. The substrates consisted of a 2.9-kbp duplex DNA containing a triplex binding site placed 15 bp in from one end and two nonoverlapping KOPS sequences placed, in permissive and nonpermissive orientations, a further 60 bp into the DNA. The DNA substrate was incubated at a ratio of 2:1 with ^{32}P 5′ end–radiolabeled 25-nucleotide triplex-forming oligonucleotide, containing a 4-nt 3′ flap, in a solution containing 25 mM MOPS (pH 5.5) and 10 mM $MgCl_2$ (ref. 35). The mixture was heated to 60 °C for 5 min and cooled to 25 °C at 1 °C min^{-1}. Triplex displacement reactions (20 µl, 22 °C) were in 50 mM HEPES (pH 7.5), 50 mM potassium glutamate, 10 mM $MgCl_2$ and 5% (w/v) glycerol. All reactions contained 1 nM triplex DNA and 250 nM FtsK and were started by the addition of ATP (to 5 mM). Reactions were stopped at 1, 2 and 5 min by addition of SDS (0.1% w/v). Displacement of triplex-forming oligonucleotide was assayed on a 1.5-mm-thick 6% (w/v) polyacrylamide gel containing TAM (40 mM Tris-acetate (pH 7.0) and 1 mM $MgCl_2$)[35].

DNA-binding reactions. DNA substrates contained overlapping triple KOPS (tKOPS) or single KOPS (sKOPS) or lacked KOPS (nKOPS). The substrates were produced by annealing appropriate oligonucleotides, one of which was ^{32}P labeled at the 5′ end, then purifying with PAGE. The binding reactions (10 µl) were carried out in 50 mM Tris (pH 8.0) buffer containing 60 mM NaCl, 1 mM EDTA, 1 mM DTT and 10% (w/v) glycerol. Radiolabeled substrate DNA (2 nM) was incubated with the protein for 5 min at 22 °C. The DNA in complex with proteins was separated from free DNA in a 6% (w/v) PAGE 0.5× TBE gel at 150 V for 2 h.

Gel filtration KOPS-binding assay. Double-stranded 16-bp DNA was assembled from HPLC-purified oligonucleotides by slow annealing. *E. coli* FtsKγ (3 mM stock) and DNA (3 mM stock) were mixed at the indicated ratios, with protein in excess, and separated on a Superdex 200 10/30 column in 20 mM Tris-HCl, 1 mM EDTA and 1 mM sodium azide (pH 7.5). Protein concentration in the purified complex was determined using BCA (Pierce) and the DNA was quantified using A_{260}.

DNA cleavage assays. *dif*-BSN substrate was ^{32}P 5′ end labeled on the top strand and was prepared as described[14]. BSN cleavage reactions were carried out under the same conditions as binding assays except that they additionally contained XerC (500 nM), XerD (250 nM) and poly(dI-dC)-poly(dI-dC) (0.125 µg ml^{-1}). Reactions were at 37 °C for 60 min and were analyzed by 6% (w/v) PAGE in 0.1% (w/v) SDS.

Accession codes. Protein Data Bank: Coordinates have been deposited with accession codes 2J5P (*E. coli* FtsKγ) and 2J5O (*P. aeruginosa* FtsKγ).

Note: Supplementary information is available on the Nature Structural & Molecular Biology website.

Table 1 NMR and refinement statistics for protein structures

	E. coli FtsK γ domain (residues 1261–1327)	*P. aeruginosa* FtsK γ domain (residues 743–809)
NMR distance and dihedral constraints		
Distance constraints		
Total NOE	1,878	1,568
Intra-residue	636	562
Inter-residue	1,242	1,006
Sequential ($\|i-j\|=1$)	389	365
Medium-range ($\|i-j\|<4$)	366	261
Long-range ($\|i-j\|>5$)	487	380
Hydrogen bonds	74	60
Total dihedral angle restraints	145	147
ϕ	59	59
ψ	59	59
$\chi 1$	27	29
Structure statistics		
Violations (mean and s.d.)		
Distance constraints (Å)	0.0093 ± 0.0005	0.0108 ± 0.0009
Dihedral angle constraints (°)	0.128 ± 0.005	0.135 ± 0.015
Max. dihedral angle violation (°)	0.102	0.142
Max. distance constraint violation (Å)	1.41	1.62
Deviations from idealized geometry		
Bond lengths (Å)	0.0018 ± 0.0001	0.0019 ± 0.0001
Bond angles (°)	0.368 ± 0.004	0.350 ± 0.012
Impropers (°)	0.29 ± 0.012	0.28 ± 0.014
Average pairwise r.m.s. deviation[a] (Å)		
Heavy	0.72 ± 0.05	0.63 ± 0.06
Backbone	0.24 ± 0.05	0.28 ± 0.08

[a]Pairwise r.m.s. deviation was calculated among the 20 lowest-energy structures without distance violations >0.25 Å or dihedral angle violations >5°.

ACKNOWLEDGMENTS

Research was supported by the Medical Research Council (Cambridge) and the Wellcome Trust (Oxford). We acknowledge our collaborators in the N.R. Cozzarelli and C. Bustamante laboratories (University of California, Berkeley) and would like to dedicate this paper to N.R. Cozzarelli, who died while this work was in progress. We thank our Oxford colleagues, P. Antrobus for his help with mass spectroscopy and I. Grainge for valuable discussions. V.S. was supported by an Oxford University Clarendon Postgraduate Award.

AUTHOR CONTRIBUTIONS

V.S., molecular biology and manuscript preparation. M.D.A., biochemistry, NMR and manuscript preparation. C.d.B., molecular biology. R.B., molecular biology. L.K.A., project direction and manuscript preparation. S.M.F., NMR. M.B., NMR. J.L., molecular biology, structural biology, project direction and manuscript preparation. D.J.S., project conception, project direction and manuscript preparation.

COMPETING INTERESTS STATEMENT

The authors declare that they have no competing financial interests.

Published online at http://www.nature.com/nsmb/
Reprints and permissions information is available online at http://npg.nature.com/reprintsandpermissions/

1. Rocha, E.P. Order and disorder in bacterial genomes. *Curr. Opin. Microbiol.* **7**, 519–527 (2004).
2. Barre, F.-X. & Sherratt, D.J. Chromosome dimer resolution. in *The Bacterial Chromosome* (ed. Higgins, N.P.) 513–524 (ASM Press, Washington, DC, 2005).
3. Wang, X., Liu, X., Possoz, C. & Sherratt, D.J. The two *Escherichia coli* chromosome arms locate to separate cell halves. *Genes Dev.* **20**, 1727–1731 (2006).
4. Blattner, F.R. *et al.* The complete genome sequence of *Escherichia coli* K-12. *Science* **277**, 1453–1474 (1997).
5. Lesterlin, C., Mercier, R., Boccard, F., Barre, F.X. & Cornet, F. Roles for replichores and macrodomains in segregation of the *Escherichia coli* chromosome. *EMBO Rep.* **6**, 557–562 (2005).
6. Ip, S.C.Y., Bregu, M., Barre, F.-X. & Sherratt, D.J. Decatenation of DNA circles by FtsK-dependent Xer site-specific recombination. *EMBO J.* **22**, 6399–6407 (2003).
7. Lesterlin, C., Barre, F-X. & Cornet, F. Genetic recombination and the cell cycle: what we have learned from chromosome dimers. *Mol. Microbiol.* **54**, 1151–1160 (2004).

© 2006 Nature Publishing Group http://www.nature.com/nsmb

8. Errington, J., Bath, J. & Wu, L.J. DNA transport in bacteria. *Nat. Rev. Mol. Cell Biol.* **2**, 538–545 (2001).
9. Saleh, O.A., Perals, C., Barre, F.-X. & Allemand, J.-F. Fast, DNA-sequence independent translocation by FtsK in a single-molecule experiment. *EMBO J.* **23**, 2430–2439 (2004).
10. Pease, P.J. *et al*. Sequence-directed DNA translocation by purified FtsK. *Science* **307**, 586–590 (2005).
11. Bigot, S. *et al.* KOPS: DNA motifs that control *E. coli* chromosome segregation by orienting the FtsK translocase. *EMBO J.* **24**, 3770–3780 (2005).
12. Levy, O. *et al*. Identification of oligonucleotide sequences that direct the movement of the *Escherichia coli* FtsK translocase. *Proc. Natl. Acad. Sci. USA* **102**, 17618–17623 (2005).
13. Wang, X., Possoz, C. & Sherratt, D.J. Dancing around the divisome: asymmetric chromosome segregation in *Escherichia coli*. *Genes Dev.* **19**, 2367–2377 (2005).
14. Yates, J. *et al*. Dissection of a functional interaction between the DNA translocase, FtsK, and the XerD recombinase. *Mol. Microbiol.* **59**, 1754–1766 (2006).
15. Massey, T.H., Mercogliano, C.P., Yates, J., Sherratt, D.J. & Löwe, J. Double-stranded DNA translocation: structure and mechanism of hexameric FtsK. *Mol. Cell* **23**, 457–469 (2006).
16. Ptacin, J.L., Nollman, M., Bustamante, C. & Cozzarelli, N.R. Identification of the FtsK-recognition domain. *Nat. Struct. Mol. Biol.,* advance online publication 15 October 2006 (doi:10.1038/nsmb1157).
17. Gajiwala, K.S. & Burley, S.K. Winged helix proteins. *Curr. Opin. Struct. Biol.* **10**, 110–116 (2000).
18. Aravind, L. *et al.* The many faces of the helix-turn-helix domain: transcription regulation and beyond. *FEMS Microbiol. Rev.* **29**, 231–262 (2005).
19. Holm, L. & Sander, C. Searching protein structure databases has come of age. *Proteins* **19**, 165–173 (1994).
20. Schwartz, T., Rould, M.A., Lowenhaupt, K., Herbert, A. & Rich, A. Crystal structure of the Za domain of the human editing enzyme ADAR1 bound to left-handed Z-DNA. *Science* **284**, 1841–1845 (1999).
21. Safo, M.K. *et al.* Structure of the MecI repressor from *Staphylococcus aureus* in complex with the cognate DNA operator, *mec*. *Acta Crystallograph. Sect. F. Struct. Biol. Cryst. Commun.* **62**, 320–324 (2006).
22. Aussel, L. *et al.* FtsK is a DNA motor protein that activates chromosome dimer resolution by switching the catalytic state of the XerC and XerD recombinases. *Cell* **108**, 195–205 (2002).
23. Singleton, M.R. *et al*. Conformational changes induced by nucleotide binding in Cdc6/ORC from *Aeropyrum pernix*. *J. Mol. Biol.* **343**, 547–557 (2004).
24. Ohnishi, T., Hishida, T., Harada, Y., Iwasaki, H. & Shinagawa, H. Structure-function analysis of the three domains of RuvB DNA motor protein. *J. Biol. Chem.* **280**, 30504–30510 (2005).
25. Oganesian, L., Moon, I.K., Bryan, T.M. & Jarstfer, M.B. Extension of G-quadruplex DNA by ciliate telomerase. *EMBO J.* **25**, 1148–1159 (2006).
26. Guzman, L.M., Belin, D., Carson, M.J. & Beckwith, J. Tight regulation modulation and high level expression by vectors containing the arabinose pBAD promoter. *J. Bacteriol.* **177**, 4121–4130 (1995).
27. Subramanya, H.S., Arciszewska, L.K., Baker, R.A., Bird, L.E., Sherratt, D.J. & Wigley, D.B. Crystal structure of the site-specific recombinase, XerD. *EMBO J.* **16**, 5178–5187 (1997).
28. Ferreira, H., Sherratt, D. & Arciszewska, L.K. Switching catalytic activity in the XerCD site-specific recombination machine. *J. Mol. Biol.* **312**, 45–57 (2001).
29. Wüthrich, K. *NMR of protein and nucleic acids* (John Wiley & Sons, New York, 1986).
30. Neri, D., Szyperski, T., Otting, G., Senn, H. & Wüthrich, K. Stereospecific nuclear magnetic resonance assignments of the methyl groups of valine and leucine in the DNA-binding domain of the 434 repressor by biosynthetically directed fractional ^{13}C labeling. *Biochemistry* **28**, 7510–7516 (1989).
31. Kraulis, P.J., Domaille, P.J., Campbell-Burk, S.L., Van Aken, T. & Laue, E.D. Solution structure and dynamics of Ras p21●GDP determined by heteronuclear three- and four-dimensional NMR spectroscopy. *Biochemistry* **33**, 3515–3531 (1994).
32. Cornilescu, G., Delaglio, F. & Bax, A. Protein backbone angle restraints from searching a database for chemical shift and sequence homology. *J. Biomol. NMR* **13**, 289–302 (1999).
33. Brünger, A.T. *et al*. Crystallography & NMR system: a new software suite for macromolecular structure determination. *Acta Crystallogr. D Biol. Crystallogr.* **54**, 905–921 (1998).
34. Recchia, G.D., Aroyo, M., Wolf, D., Blakely, G. & Sherratt, D.J. FtsK-dependent and -independent pathways of Xer site-specific recombination. *EMBO J.* **18**, 5724–5734 (1999).
35. Firman, K. & Szczelkun, M.D. Measuring motion on DNA by the type I restriction endonuclease EcoR124 using triplex displacement. *EMBO J.* **19**, 2094–2102 (2000).

© 2006 Nature Publishing Group http://www.nature.com/nsmb